Journal of Power Sources 184 (2008) 375–380

Contents lists available at ScienceDirect

Journal of Power Sources

journal homepage: www.elsevier.com/locate/jpowsour

Short communication

Nanostructured polypyrrole/carbon composite as Pt catalyst support for fuel cell applications

Hongbin Zhao, Lei Li*, Jun Yang**, Yongming Zhang

School of Chemistry and Chemical Technology, Shanghai Jiao Tong University, Shanghai 200240, China

ARTICLE INFO

Article history:
Received 2 January 2008
Received in revised form 23 February 2008
Accepted 17 March 2008
Available online 22 March 2008

Keywords:
Polypyrrole
Composite support
Fuel cell
Electrocatalysis

ABSTRACT

A novel catalyst support was synthesized by *in situ* chemical oxidative polymerization of pyrrole on Vulcan XC-72 carbon in naphthalene sulfonic acid (NSA) solution containing ammonium persulfate as oxidant at room temperature. Pt nanoparticles with 3–4 nm size were deposited on the prepared polypyrrole–carbon composites by chemical reduction method. Scanning electron microscopy and transmission electron microscopy measurements showed that Pt particles were homogeneously dispersed in polypyrrole–carbon composites. The Pt nanoparticles-dispersed catalyst composites were used as anodes of fuel cells for hydrogen and methanol oxidation. Cyclic voltammetry measurements of hydrogen and methanol oxidation showed that Pt nanoparticles deposited on polypyrrole–carbon with NSA as dopant exhibit better catalytic activity than those on plain carbon. This result might be due to the higher electrochemically available surface areas, electronic conductivity and easier charge-transfer at polymer/carbon particle interfaces allowing a high dispersion and utilization of deposited Pt nanoparticles.

1. Introduction

Fuel cells, as devices for direct conversion of the chemical energy of a fuel into electricity by electrochemical reactions, are among the key enabling technologies for the transition to a hydrogen-based economy [1–3]. Direct methanol fuel cells (DMFCs) have been attracting enormous research interest as portable power sources because of their high energy density, fuel portability, and low operating temperature [4,5]. However, poor methanol oxidation at the anode is one of the main challenges to develop DMFC applications. The poor methanol oxidation is the sluggish electrochemical oxidation of adsorbed carbon monoxide, an intermediate of the anodic methanol oxidation. To improve the anode catalyst performance, a major strategy is to develop supporting materials to achieve high dispersion, utilization, activity, and stability for catalysts [6,7]. This approach is particularly important for lowering the fuel cell cost by reducing the use of expensive Pt-based noble metal catalysts. A suitable supporting material must be stable in acid media, good electronic conductivity, and high specific surface area. An anisotropic morphology is helpful to improve mass transport properties in the catalyst layer. By suitably combining conducting polymer and carbon with catalytic metal nanoparticles, new electrocatalysts with higher surface area and methanol oxidation activity can be generated [8].

Conducting polymers, such as polyaniline (PANi) and polypyrrole (PPy), having good electronic and proton conductivity, dispensability and special nanometer structure, have attracted much attention for fuel cell applications [9–15]. PPy is unique among the family of conjugated polymers since its doping level can be readily controlled through an acid doping/base de-doping process [16–19]. It has been shown that the use of macromolecule proton acid as a dopant can enhance the electronic conductivity of PPy and limit the growth of PPy particles [20–22]. Owning to its high conductivity and environmental stability, PPy has been extensively studied in many fields, including anticorrosion coating, second battery anode material, sensors, medical materials, electromagnetic shielding devices and solid electrolyte condenser [23,24].

Recently, *in situ* chemical polymerization method has been used to prepare nanosized powder, wire, fiber and tube of PPy broadly, in which $FeCl_3$, $(NH_4)_2S_2O_8$ or H_2O_2 were used as oxidant and HCl or H_2SO_4 as proton acid [9,25–27]. For fuel cell application, it is expected that PPy-modification can increase the electrochemical surface area and improve the electrocatalysis ability of Pt/carbon catalyst. Here, we prepared the nanostructured PPy–carbon composite as an electrocatalyst support and research the effect of

* Corresponding author. Tel.: +86 21 34202613.
** Corresponding author. Tel.: +86 21 54747667; fax: +86 21 54747667.
E-mail addresses: lilei0323@yahoo.com.cn (L. Li), yangj723@sjtu.edu.cn (J. Yang).

0378-7753/$ – see front matter © 2008 Elsevier B.V. All rights reserved.
doi:10.1016/j.jpowsour.2008.03.024

naphthalene sulfonic acid as dopant on the electrochemical oxidation of hydrogen and methanol.

2. Experimental

2.1. Materials

Reagent grade β-naphthalene sulfonic acid (NSA), sodium borohydride ($NaBH_4$) and ammonium persulfate (APS) were obtained from China National Pharmaceutical Group Corp., and catalyst precursor salt $H_2PtCl_6{\cdot}6H_2O$ was purchased from Alfa Aesar. Chemically pure pyrrole (Py) monomer was obtained from Sinopharm Chemical Reagent Co. Ltd. Double-distilled (DDI) water was used throughout the experiments.

Vulcan XC-72 carbon powder from Cabot Company was pretreated with 6 M HNO_3 and DDI water at 100 °C, respectively. Then it was washed with DDI water and dried at room temperature under vacuum condition for 24 h.

2.2. Synthesis of polypyrrole–carbon composite

Polypyrrole–carbon composites were synthesized by *in situ* chemical oxidative polymerization of Py monomer on carbon powders. 150 mL ethanol solution containing Vulcan XC-72 (0.6 g) was sonicated at room temperature for 0.5 h to disperse carbon powder. Py monomer (3 mmol) solved in 100 mL DDI water was added to the above suspension solution and keep stirring for 30 min. Then 100 mL APS (6 mmol) solution containing NSA (0.001 mol, the Py/NSA molar ratio according to the Ref. [28] is 3:1) was added slowly to the suspension with constant stir for 4 h at room temperature. After reaction, the resulting PPy–XC72 powder was filtered and rinsed with distilled water and ethanol until the filtrate became colorless. The obtained black powder was dried under vacuum condition at room temperature for 24 h. For comparison, the PPy–XC72 without NSA was prepared by the same method.

2.3. Synthesis of Pt nanoparticle decorated polypyrrole/carbon composites (40 wt.% Pt/PPy–XC72)

40 wt.% Pt/PPy–XC72 catalysts were prepared by chemical reduction method. 100 mg PPy–XC72 support was suspended in 10 mL DDI water, then stirred using ultrasonic treatment for 20 min and then mechanically stirred for 4 h. 3 mg mL^{-1} H_2PtCl_6 aqueous solution was dropped to the PPy–XC72 suspension solution. A flow of nitrogen was passed through the reaction system to isolate oxygen. Pt particles were deposited onto the PPy–XC72 support by adding 200 mL $NaBH_4$ (0.05 mg mL^{-1}) of ethanol solution for 3 h to the solution at room temperature. The resulting catalyst particles were then filtered and washed with de-ionized water, and finally dried at 45 °C for 12 h. A similar procedure was followed to synthesize 40 wt.% Pt/PPy–XC72 without NSA as dopant and Pt/carbon catalysts. The platinum loading in the catalyst were 40 wt.% in our experiments.

2.4. Fabrication of 40% Pt/PPy–XC72 electrodes

Catalyst ink was prepared by blending 40 wt.% Pt/PPy–XC72 catalyst with ethanol and 5 wt.% perfluorosulfonic acid (PFSA) ionomer solution (Dongyue Group Co Ltd., China). 5 mg catalyst was added into 10 mL ethyl alcohol and 0.5 mL of 5 wt.% PFSA solution, and ultrasonically mixed for 30 min. Then, 30 μL mixed solution was uniformly dispersed on glassy carbon electrode and dried at room temperature. In our experiments, the weight ration of PFSA and catalyst was 1:2.

2.5. Characterization

The SEM and TEM images were taken using JEM-100CX scanning electron microscope and JEOL S-520 transmission electron microscopy, respectively. X-ray diffraction (XRD) experiments were carried out on D/max-2200/PC X-ray Diffractometer. The electronic conductivity of catalyst was measured by four-probe conductivity measurement method.

Cyclic voltammeter measurements were carried out in a three-electrode cell by using a Model 616 rotating disk electrode from Autolab PGSTAT302 electrochemical test system (Eco Chemie, Netherland). A glassy carbon disk (3 mm o.d.) coating catalyst was used as working electrode, a platinum foil as counter-electrode, and an Ag/AgCl electrode as reference. 0.5 M H_2SO_4 aqueous solution served as electrolyte for hydrogen oxidation measurements, and 0.5 M H_2SO_4 + 1 M CH_3OH aqueous solution for methanol oxidation measurements, respectively. High-purity N_2 was bubbled into the electrolytes during the experiment.

The CO stripping test was carried out as follows. CO was adsorbed by flowing pure CO at a flow rate of 100 mL min^{-1} through the 0.5 M H_2SO_4 aqueous solution for 30 min, while holding the electrode potential at 0.1 V. By keeping the potential at the same value the gas was switched to N_2 for 15 min and remove CO traces from the gas phase. After additional 20 min, the potential was scanned with the sweep rate of 20 mV s^{-1} from the starting potential to 1.0 V and then back to −0.3 V.

3. Results and discussion

The stereo structure of electrodes is an important property of fuel cell, in which carbon is considered to supply good electronic conductivity, and PFSA provides proton transfer channels. Therefore, the surfaces with the contact among platinum, carbon and PFSA become a key to assess the property of electrode. Furthermore, how to improve the space structure of these three phases is also very important. While polypyrrole is introduced to this space structure as a proton conductive polymer material, the electrochemical performance of electrode may be improved.

The geometric configurations of both nanostructured PPy–XC72 electro-catalytic supports with and without NSA dopant are shown in Fig. 1. It is difficult to identify and distinguish carbon and polypyrrole particles. The polypyrrole/carbon composite consists of agglomerate particles with the primary particle size of about 20–30 nm. These agglomerate particles are made up of homogeneous clusters with about 100–200 nm. Carbon particles and polypyrrole seem not to be mechanically mixed but well incorporate each other. Maybe such a good dispersion will supply a good transfer channel for proton and electron, and reduce the electric resistance of phase interface. The average particle size of the nanostructured PPy–carbon composites prepared with NSA concentrations of 0.005, 0.02 and 0.1 M as dopant is about 20, 21 and 25 nm, respectively. A conjecture for the particle size difference is that different PPy structure. Structurally, most of the PPy units without dopant should be a long and line arrangement. When NSA was added as a dopant, one molecule of NSA will dope with three pyrrole rings [28], and the line morphology will be changed, hence the decrease of particle size of PPy. But redundant NSA will be wrapped in the PPy matrix, which will make the PPy–XC72 particle size large.

Fig. 2 shows the TEM images of platinum deposited on the surface of PPy–XC72 composite supports. It can be seen that well dispersed, spherical platinum particles were anchored on the surface of PPy–XC72 composite supports with size ranging from 3 to 4 nm, be comparable with that of JM commercial 40% Pt/C (<4.5 nm)

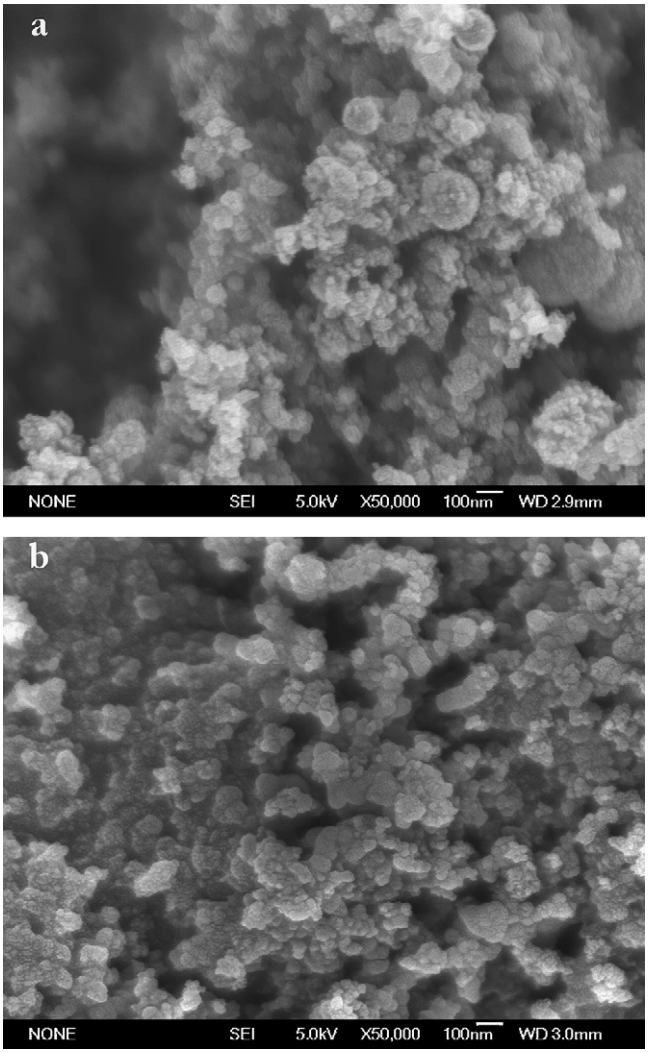

Fig. 1. SEM images of PPy–XC72 with (a) and without (b) NSA as dopant.

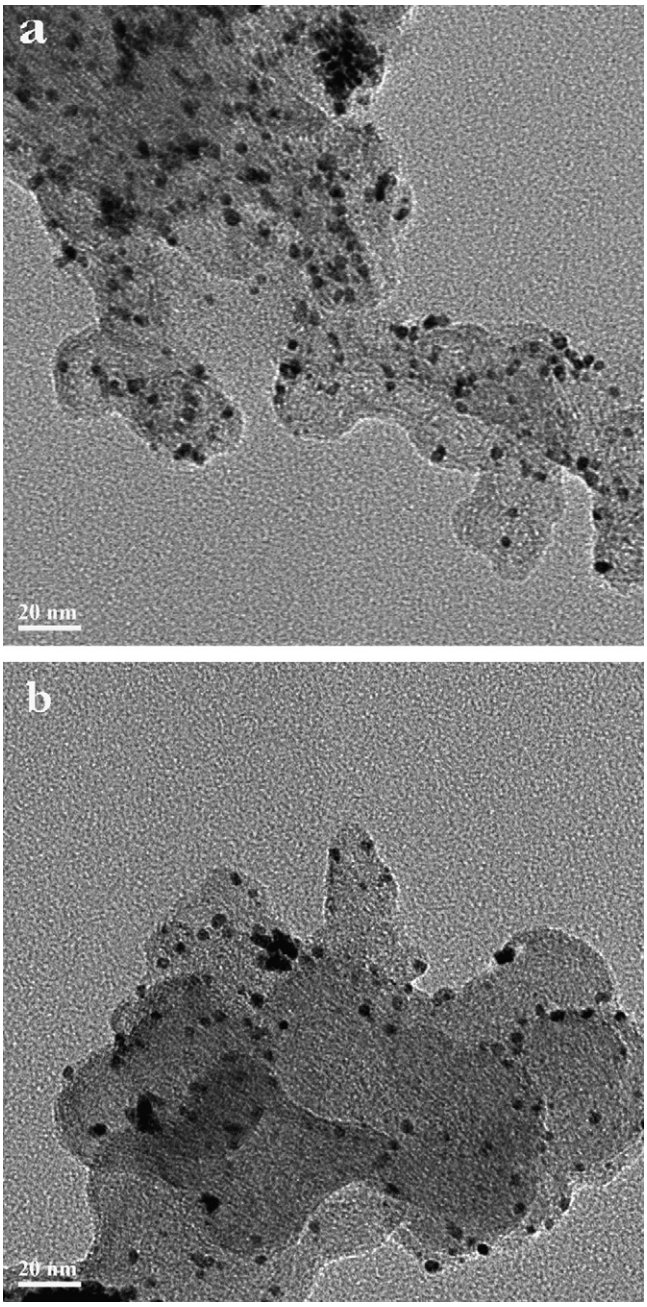

Fig. 2. TEM images of Pt/PPy–XC72 with (a) and without (b) NSA as dopant.

[29]. The nanosized Pt dispersion on PPy–XC72 composites provides a favorable condition for good electrochemical performance.

In order to research the effects of PPy and NSA on the conductivity of catalyst support, the conductivities of different catalyst supports were measured via four-probe conductivity measurement method. The test result (Table 1) shows that the pretreated XC72 carbon black has a high conductivity about 28 S cm^{-1}, and the conductivity of PPy–XC72 with and without NSA as dopant is 25.9 and 12 S cm^{-1}, respectively. The conductivity of PPy–XC72 with NSA as dopant is high enough to provide electrons transfer channel. While comparing both the PPy–XC72 composite supports, we find that the additional NSA as dopant plays an important role in improving the conductivity of PPy–XC72. A high conductivity of PPy–XC72 with NSA as dopant should be due to that NSA, as a macromolecule acid, can dope into the 3D structure of PPy matrix and form a proton acid structure, which improve the ability of electronic transfer. So in this paper, by NSA as dopant, the composite support still keeps a high conductivity and is suitable to be used as a catalyst support. Also to some content, such a method can improve the stereo structure of catalyst layer and should be an effective method in carbon modification.

Table 1
The conductivity of different catalyst supports

Catalyst support	Conductivity (S cm^{-1})
XC72	28
PPy–XC72 without NSA as dopant	12
PPy–XC72 with NSA as dopant	25.9

The XRD patterns of 40% Pt/PPy–XC72 with and without NSA dopant are shown in Fig. 3. The first peak located at about 26.3° corresponds to characteristic of graphite (0 0 2) plate of the PPy–XC72 support. The three peaks at 2θ values of about 39.7°, 46.2° and 67.5° are characteristic of face-centered cubic (fcc) crystalline Pt (JCPDS, Card no. 04-0802), referred to the planes (1 1 1), (2 0 0) and (2 2 0) [30,31]. In view of that the (2 2 0) peak is not affected by carbon and PFAS, the average size of the Pt particles on PPy–XC72 with and without dopant are calculated from Pt(2 2 0) peak by means of the Scherrer formula. It is estimated from the Scherrer formula that the

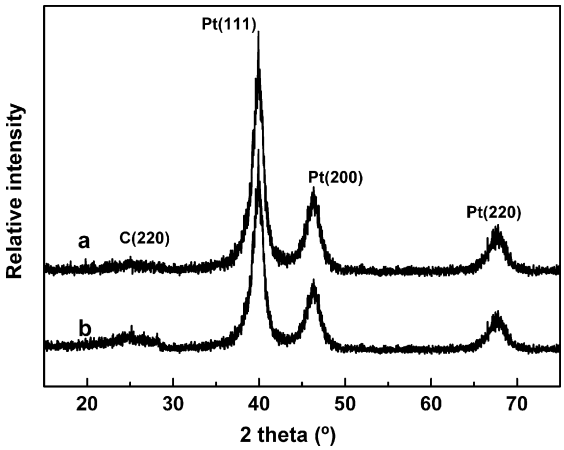

Fig. 3. X-ray diffraction of 40% Pt/PPy–XC72 with (a) and without (b) NSA as dopant.

average size of Pt particles on PPy–XC72 with and without dopant is 3.3 and 3.6 nm, respectively. These values are consistent with the result observed from the TEM images. All of these two catalysts have the high and sharp peak, which means that the Pt(1 1 1) is perfect. But the XRD of Pt/PPy–XC72 with NSA as dopant has wider half peak, indicating smaller particle size. The finer particle dispersion can provide more Pt catalysis sites and thus improve the hydrogen reduction ability. It is beneficial for accelerating the oxidation speed of hydrogen, thus improve the catalysis activity.

The electrochemical stability of the composite supports was studied by an additional CV experiment with the composite support modified glassy carbon electrode as work electrode in H_2SO_4 aqueous solution. In the CV curves (Fig. 4), these two composite supports have the identical shape and no other reactions when the NSA was added into the composite support, which confirms that the PPy–XC72 with NSA as dopant is electrochemically stable in the potential range from −0.3 to 1.0 V.

The electrochemical reactivity and electrochemical active surface areas of different catalysts were determined by cyclic voltammetry measurement performed in 0.5 M H_2SO_4 aqueous solution at a sweep rate of 20 mV s^{-1}. As shown in Fig. 5, the hydrogen adsorption and desorption peaks of Pt/PPy–XC72 with NSA as dopant (a) are bigger than those of the other two electrochemical catalysts. According to the columbic amount (Q) associated with

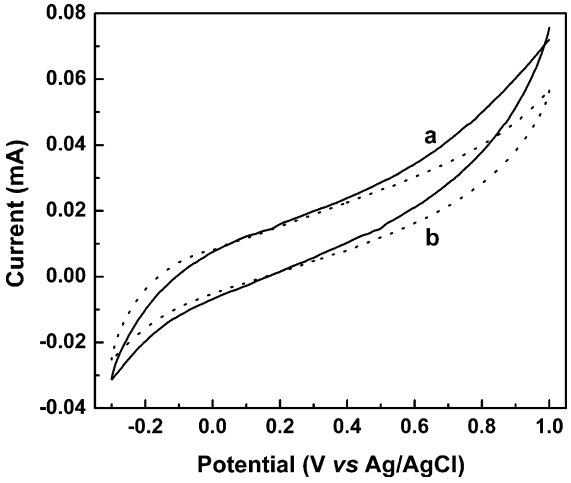

Fig. 4. Cyclic voltammograms of PPy–XC72 with (a) and without (b) NSA as dopant on glassy carbon electrode, electrolyte: 0.5 M H_2SO_4, sweep rate: 20 mV s^{-1} and temperature: 25 °C.

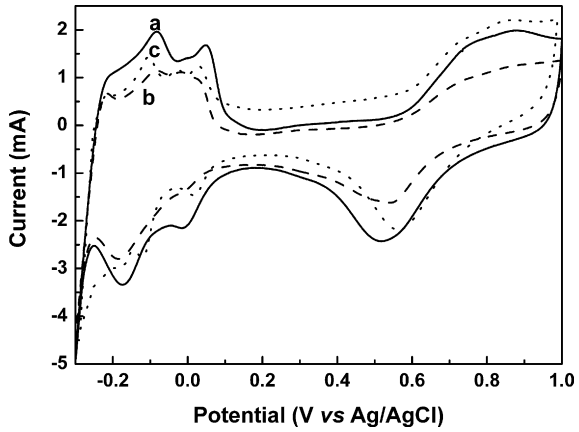

Fig. 5. Cyclic voltammograms of 40% Pt/PPy–XC72 with (a) and without (b) NSA as dopant and commercial 40% Pt/C (c), electrolyte: 0.5 M H_2SO_4 aqueous solution, sweep rate: 20 mV s^{-1}, temperature: 25 °C and Pt loading: 200 μg cm^{-2}.

the peak area, the electrochemically active surface (EAS) can be calculated using the following equation [32,33]:

$$\mathrm{EAS} = \frac{Q}{m \cdot C}$$

where C denotes the quantity of electricity when hydrogen molecules adsorb on platinum with a homogenous and single layer, here it is 210 μC cm^2, m is the mass of platinum on catalyst surface.

The EAS values of the catalysts are shown in Table 2. The EAS value of our catalyst with NSA (85 m^2 g^{-1} Pt) is larger than that without NSA (68 m^2 g^{-1} Pt) and JM commercial 40% Pt/C (62 m^2 g^{-1} Pt). Moreover, it is noticed from Fig. 5 that both the Pt/PPy–XC72 catalysts present identical hydrogen oxidation potential compared with JM commercial 40% Pt/C. It means that the PPy–XC72 composite support also supplied the good electron conductivity by introducing PPy as a support component. Here, the finely dispersed mixed-conducting PPy may act as an intermediate to connect electrically conducting carbon and proton-conducting PFSA and ensure a better compatibility among the different components. Therefore, an effective conducting network for the transportation of both electron and proton may be established. This may be the important reason for the significant improvement in the electrochemical performance.

The methanol electrocatalytic activity of Pt/PPy–XC72 with NSA as dopant was evaluated by the electrochemical oxidation of CH_3OH. For comparison, Pt/PPy–XC72 without NSA as dopant and JM commercial Pt/C catalyst were also compared at the same condition.

The reaction mechanism for methanol oxidation may be suggested as follows [34]:

$$CH_3OH + Pt \rightarrow Pt{-}CH_2OH + H^+ + e^- \quad (1)$$

$$Pt{-}CH_2OH + Pt \rightarrow Pt_2{-}CHOH + H^+ + e^- \quad (2)$$

$$Pt_2{-}CHOH + Pt \rightarrow Pt_3{-}COH + H^+ + e^- \quad (3)$$

$$Pt_3{-}COH + Pt \rightarrow Pt{-}(CO)_{ad} + 2Pt + H^+ + e^- \quad (4)$$

Table 2
Electrochemical active surface of different catalysts

Catalyst	EAS (m^2 g^{-1} Pt)
Pt/PPy–C with NSA as dopant	85
Pt/PPy–C without dopant	86
JM commercial 40% Pt/C	62

Determined from the hydrogen adsorption/desorption region of the CV curves in 0.5 M H_2SO_4 aqueous solution.

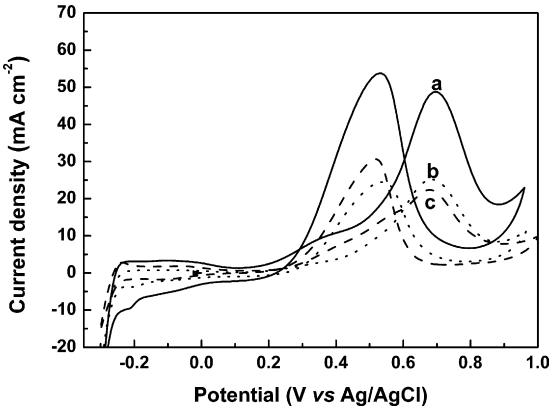

Fig. 6. Cyclic voltammograms of 40% Pt/PPy–XC72 with (a) and without (b) NSA as dopant and commercial 40% Pt/C (c), electrolyte: 0.5 M H_2SO_4 + 1 M CH_3OH aqueous solution, sweep rate: 20 mV s^{-1}, temperature: 25 °C and Pt loading: 200 μg cm^{-2}.

$$Pt + H_2O \rightarrow Pt{-}(OH)_{ad} + H^+ + e^- \quad (5)$$

$$Pt{-}(CO)_{ad} + Pt{-}(OH)_{ad} \rightarrow CO_2 + H^+ + e^- + 2Pt \quad (6)$$

The overall reaction can be expressed as

$$CH_3OH \rightarrow Pt{-}(CO)_{ad} + 4H^+ + 4e^- + H_2O \rightarrow CO_2 + 6H^+ + 6e^- \quad (7)$$

In this methanol mechanism, the intermediate CO_{ad} adsorbed on the surface of Pt to form $Pt{-}(CO)_{ad}$ (4). Because the binding energy of $Pt{-}(CO)_{ad}$ is very strong, CO_{ad} is difficult to desorbed from Pt, the whole layer of $Pt{-}(CO)_{ad}$ on the surface of Pt will decrease the EAS of Pt. We note that the $Pt{-}(OH)_{ad}$ is the only intermediate which play the function of methanol oxidation, and it is required that CO diffuse to the surface of the places where the $(OH)_{ad}$ is formed [35]. More amount of $Pt{-}(OH)_{ad}$ is benefit to accelerate the $Pt{-}(CO)_{ad}$ to be oxidized to CO_2. Without enough active Pt particles, the methanol oxidation will be limited seriously.

As shown in Fig. 6, the two strong oxidation peaks belong to methanol oxidation. The onset potential for methanol oxidation of Pt/PPy–XC72 with NSA as dopant shows a negative shift with a higher peak current density compared to that of JM commercial Pt/C and Pt/PPy–XC72 without NSA as dopant, which means that methanol is easier to be oxidized on the surface of Pt/PPy–XC72 with NSA as dopant than other two catalysts. The large methanol oxidation peak density means that the $Pt{-}(OH)_{ad}$ is easier to form on Pt/PPy–XC72 with NSA as dopant than on another two catalysts. More amounts of $Pt{-}(OH)_{ad}$ will react with the intermediate $Pt_3{-}COH_{ads}$ to form carbon dioxide, and improve the methanol oxidation speed. The high positive oxidation peak and relatively low oxidation potential indicates the excellent methanol oxidation ability of the Pt/PPy–XC72 with NSA as dopant.

The CO stripping experiment was carried out to check the CO poisoning on our catalyst. From the CV of CO stripping test (Fig. 7), it is observed that after the second anodic sweep, all the CO oxidation peaks disappear. It means that these three catalysts can oxidize CO completely. The CO oxidation peak potentials on Pt/PPy–XC72 with and without NSA are at 0.56 and 0.57 V versus Ag/AgCl, while the CO stripping peak potential is 0.71 V for the commercial Pt/C catalyst. Both CO stripping peak potential of Pt/PPy–XC72 with NSA as dopant and the onset CO oxidation potential are more negative than that of commercial catalyst. The CO stripping test result gives us a proof that the Pt/PPy–XC72 with NSA as dopant has potential for CO-tolerant anode catalyst in DMFCs. One reason for the good CO-tolerant ability of Pt/PPy–XC72 with NSA as dopant is that the interaction between the Pt particles and PPy may inhibit the formation of strongly chemisorbed species, which prevents the Pt catalytic site to be poisoned and thus leads to higher activity and

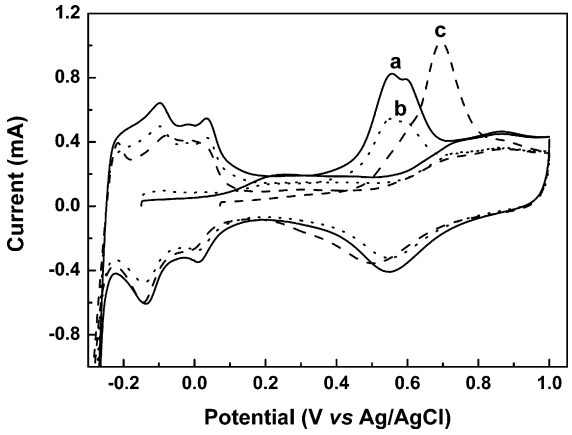

Fig. 7. CO stripping voltammetry of 40% Pt/PPy–XC72 with (a) and without (b) NSA as dopant and commercial Pt/C (c) after CO adsorption at 0.1 V vs. Ag/AgCl for 30 min, pure CO saturated for 15 min, electrolyte: 0.5 M H_2SO_4, sweep rate: 50 mV s^{-1} and room temperature.

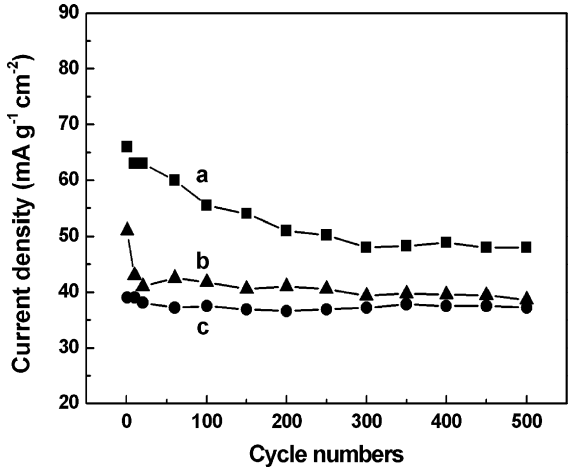

Fig. 8. Long-term stability of 40% Pt/PPy–XC72 with (a) and without (b) NSA as dopant and JM commercial 40% Pt/C (c) electrodes in 0.5 M H_2SO_4 + 1 M CH_3OH aqueous solution and sweep rate: 20 mV s^{-1}.

greater stability for methanol oxidation. It is similar to the report that oxidation of methanol at the Pt modified polypyrrole GC electrode [36].

The long-term stability of 40% Pt/PPy–XC72 with NSA as dopant was further studied in 0.5 M H_2SO_4 + 0.5 M CH_3OH aqueous solution with a scan ate is 20 mV s^{-1}. As shown in Fig. 8, before 300 cycles, the peak current density of Pt/PPy–XC72 with NSA as dopant fall down slowly, the reason should be that the different support structure, which affects the transfer of methanol and intermediate species, the methanol diffusion control step. Before 300 cycles, the diffusion speed of methanol into the catalyst is faster than that of intermediate products diffuse out of catalyst layer. These two diffusion speeds are not accordant, so before 300 cycles, there is a slow decrease of peak density. After 300 cycles, the two diffusion processes arrived at a balance. The anodic peak density shows a stable density about 15.8 mA cm^{-2}. It should be due to the diffusion balance of methanol and intermediate species, and the methanol oxidation speed trend to be stable. After 500 cycles of CV test, the current density of anodic peak on 40% Pt/PPy–XC72 (NSA as dopant) catalyst electrode is about 50.8 mA cm^{-2} higher than the commercial 40% Pt/C catalyst.

4. Conclusions

Polypyrrole/Vulcan XC72 carbon composite was prepared by *in situ* chemical oxidative polymerization of pyrrole monomer on carbon particles. SEM measurements show that the polypyrrole–carbon composite has a homogeneous primary particle distribution from 20 to 30 nm. TEM measurements confirm that platinum nanoparticles, with a size range of 3–4 nm, are well deposited on the polypyrrole–carbon support. Judging from peak current densities and onset potentials of cyclic voltammograms, the Pt/PPy–XC72 composite with NSA as dopant has excellent electrochemical catalytic activity for hydrogen and methanol oxidation. Nanostructured and mixed-conducting PPy as a component of Pt catalyst support is favorable for setting up an effective conducting network for electron and proton transportation and may improve the surface morphology for platinum deposition. NSA doping in the PPy–XC72 support could further enhance the conducting ability of the catalyst layer. These are the possible reasons for the improvement in the hydrogen and methanol oxidation ability. Moreover, the CO stripping experiment affirms that the 40 wt.% Pt/PPy–XC72 has good CO-tolerant ability. In addition, the composite catalyst of 40 wt.% Pt/PPy–XC72 with NSA shows the long-term stability in CH_3OH-containing solution. After 500 cycles, the peak current density remains higher than the commercial catalyst. On the other hand, it needs to be investigated whether there is some special interaction between nanosized platinum and the PPy–XC72 composite, which leads to the enhanced electrochemical activation.

Acknowledgement

This work is financial supported by the key technology R&D under contract 2006BAE02A04, China.

References

[1] B. Rajesh, K. Ravindranathan Thampi, J.M. Bonard, H.J. Mathieu, N. Xanthopoulos, B. Viswanathan, Electrochem. Solid-State Lett. 7 (2004) 404–410.
[2] B. Rajesh, Z. Piotr, Nature 443 (2006) 63–71.
[3] T.D. Jarvi, S. Sriramulu, E.M. Stuve, Colloids Surf. 134 (1998) 152–158.
[4] R. Dillon, S. Srinivasan, A.S. Arico, V. Antonucci, J. Power Sources 127 (2004) 112–126.
[5] A.S. Arico, V. Baglio, E. Modica, A. Blasi, V. Antonucci, Electrochem. Commun. 6 (2004) 164–169.
[6] M. Uchida, Y. Aoyama, M. Tanabe, N. Yanagihara, N. Eda, A. Ohta, J. Electrochem. Soc. 142 (1995) 2572–2576.
[7] G. Wu, Y.S. Chen, B.Q. Xu, Electrochem. Commun. 7 (2005) 1237–1243.
[8] V. Selvaraj, M. Alagar, K. Sathish Kumar, Appl. Catal. B: Environ. 75 (2007) 129–138.
[9] Y. Shen, M. Wan, J. Polym. Sci. A: Polym. Chem. 37 (1999) 1443–1451.
[10] D.H. Reneker, I. Chun, Nanotechnology 7 (1996) 216–223.
[11] R. Dersch, M. Steinhart, U. Boudriot, A. Greiner, J.H. Wendorff, Polym. Adv. Technol. 16 (2005) 276–282.
[12] T. Ochi, Biochem. Biophysic. Res. Commun. 11 (2004) 67–70.
[13] C.R. Martin, Acc. Chem. Res. 28 (1995) 61–68.
[14] M.J. Sailor, C.L. Curtis, Adv. Mater. 6 (1994) 688–692.
[15] G.G. Wallace, P.C. Innis, J. Nanosci. Nanotechnol. 2 (2002) 441–451.
[16] J.X. Huang, R.B. Kaner, Chem. Commun. (2006) 367–376.
[17] W.S. Huang, B.D. Humphrey, A.G. Mac Diarmid, J. Chem. Soc., Faraday Trans. 1 (1986) 2385–2400.
[18] A.G. MacDiarmid, J.C. Chiang, M. Halpern, W.S. Huang, S.L. Mu, N.L.D. Somasiri, W.Q. Wu, S.I. Yaniger, Mol. Cryst. Liq. Cryst. 121 (1985) 173–180.
[19] A.G. MacDiarmid, Synth. Met. 84 (1994) 27–34.
[20] Y. Cao, P. Smith, A.J. Heeger, U.S. Patent 5,624,605 (1997).
[21] Y. Cao, P. Smith, A.J. Heeger, Synth. Met. 55 (1993) 3514–3519.
[22] J. Su, G.C. Wang, H.S. Deng, X.Q. Fan, J. Funct. Polym. 15 (2002) 122–125.
[23] P. Chandrasekhar, Conducting Polymers, Fundamentals and Applications: A Practical Approach, Kluwer Academic Publishers, Boston, 1999, pp. 351–398.
[24] T.J. Skotheim, R.L. Elsenbaumer, J.R. Reynolds, Handbook of Conducting Polymers, Marcel Dekker, New York, 1998, pp. 1–120.
[25] V. Selvaraj, M. Alagar, Electrochem. Commun. 9 (2007) 1145–1153.
[26] Y.C. Liu, C.J. Tsai, J. Electroanal. Chem. 537 (2002) 165–173.
[27] S. Sinharay, M. Biswas, Mater. Res. Bull. 34 (1999) 1187–1193.
[28] K. Diez, B. Tauer,. Schulz, Colloid. Polym. Sci. 283 (2004) 125–132.
[29] http://www.jmfuelcells.com/HiSPEC_Customer_Chart.pdf.
[30] T. Swanson, E. Tatge, Natl. Bur. Stand. (U.S.) Circ. 539 (1953) 31–32.
[31] G. Harcourt, Am. Mineral. 84 (1942) 667–789.
[32] J. Fournier, G. Fuabert, J.Y. Tilquin, J. Electrochem. Soc. 144 (1997) 145–154.
[33] K.W. Park, J.H. Choi, K.S. Ahn, J. Phys. Chem. B 108 (2004) 5989–5994.
[34] E. Leiva, C. Sánchez, in: V. Wolf, L. Arnold, G. Hubert (Eds.), Handbook of Fuel Cells: Fundamentals Technology and Applications, John Wiley & Sons Ltd., New Jersey, 2005, pp. 93–130.
[35] T.I. wasita, Handbook of Fuel Cells: Fundamentals Technology and Applications, Electrocatalysis, John Wiley & Sons Ltd., 2003.
[36] J. Li, X.Q. Lin, J. Electrochem. Soc. 154 (2007) 1074–1079.